

17 Apr 2004, 10:30am - 12:30pm

## Field Verification of the Energy-Based Procedure to Predict the Liquefaction Potential of Soil Deposits

M. Tao

Case Western Reserve University, Cleveland, Ohio

J. L. Figueroa

Case Western Reserve University, Cleveland, Ohio

A. S. Saada

Case Western Reserve University, Cleveland, Ohio

Follow this and additional works at: <https://scholarsmine.mst.edu/icchge>



Part of the [Geotechnical Engineering Commons](#)

### Recommended Citation

Tao, M.; Figueroa, J. L.; and Saada, A. S., "Field Verification of the Energy-Based Procedure to Predict the Liquefaction Potential of Soil Deposits" (2004). *International Conference on Case Histories in Geotechnical Engineering*. 1.

<https://scholarsmine.mst.edu/icchge/5icchge/session03/1>



This work is licensed under a [Creative Commons Attribution-Noncommercial-No Derivative Works 4.0 License](#).

This Article - Conference proceedings is brought to you for free and open access by Scholars' Mine. It has been accepted for inclusion in International Conference on Case Histories in Geotechnical Engineering by an authorized administrator of Scholars' Mine. This work is protected by U. S. Copyright Law. Unauthorized use including reproduction for redistribution requires the permission of the copyright holder. For more information, please contact [scholarsmine@mst.edu](mailto:scholarsmine@mst.edu).



## FIELD VERIFICATION OF THE ENERGY-BASED PROCEDURE TO PREDICT THE LIQUEFACTION POTENTIAL OF SOIL DEPOSITS

**M. Tao**

Dept. of Civ. Engrg.  
Case Western Reserve Univ.  
Cleveland-USA-44106

**J. L. Figueroa**

Dept. of Civ. Engrg.  
Case Western Reserve Univ.  
Cleveland-USA-44106

**A. S. Saada**

Dept. of Civ. Engrg.  
Case Western Reserve Univ.  
Cleveland-USA-44106

### ABSTRACT

This paper presents field evidence in support of the energy-base procedure to predict the liquefaction potential of soil deposits. Two recorded earthquake events which occurred at the Wildlife Site: Elmore Ranch earthquake (11/23/1987) and Superstition Hills earthquake (11/24/1987), representing nonliquefaction and liquefaction case histories respectively, were utilized to verify the energy-based procedure in field situations. The nonlinearity and the degradation of shear stiffness and strength of soil deposits subjected to earthquake loading under undrained conditions were incorporated in the reconstruction of the shear stress-stain response. The effects of multi-directional excitation on the liquefaction potential and the build-up of pore water pressure were also investigated. Finally, a unit energy-pore pressure model was confirmed by the comparison of the calculated and recorded pore pressure time histories.

### INTRODUCTION

As a relatively new method, the energy-based procedure to evaluate the liquefaction potential of soils has been proven successful and promising in the laboratory (Liang et al., 1995; Dief 2000). However, less confirmation in field situations has been presented, which has resulted in its rare application to engineering practice.

A step-by-step procedure is introduced to facilitate the application of the energy-based procedure developed at Case Western Reserve University. The liquefaction resistance of soils in this procedure can be experimentally determined; while the amount of energy dissipated into soils during a potential earthquake is assessed by a modified numerical procedure. Based on two recorded downhole array data, field verification is performed. The validity of the energy-based procedure is confirmed by the successful field verification. In addition, the effect of multi-dimensional loading on the liquefaction potential of soils is investigated.

### A STEP-BY-STEP PROCEDURE TO DETERMINE THE LIQUEFACTION POTENTIAL OF SOILS

Either cyclic shear stress or shear strain was used as criterion of the liquefaction failure in the stress-based or strain-based procedures. Similarly, the unit energy is chosen to be a criterion in the energy-based procedures. A tentative step-by-step procedure to determine the liquefaction potential of soils

introduced by Liang (Liang, 1995) is used in this paper and can be summarized as follows.

#### 1. Determination of the liquefaction resistance in terms of the unit energy

As a measure of the liquefaction resistance of soils, the cumulative unit energy has been proven heavily dependent on fabric characteristics, relative density and stress state of soils, but relatively independent of loading characteristics (loading frequency, loading patterns, and loading paths) or testing procedures (Tao et al. 2003). Therefore, any commonly used geotechnical dynamic testing procedure, such as cyclic triaxial test, cyclic simple shear test, cyclic torsional shear test, and centrifuge test, could be conducted on reconstituted or undisturbed samples of soils procured from the site under investigation. It is to be noted that the range of the confining pressure and relative densities used in tests should cover all the states of the soils present in the field.

If the soil at the site under investigation is similar to those tested at Case Western Reserve University, the regression relationships given in Eqs. (1)-(5) could be used to approximate the cumulative dissipated unit energy.

*For Reid Bedford Sand (Liang, 1995):*

$$\log_{10}(\delta w) = 2.002 + 0.00477\sigma'_c + 0.0116D_r, R^2 = 0.937 \quad (1)$$

*For LSI30 sand (Liang, 1995):*

$$\log_{10}(\delta w) = 2.0554 + 0.004824\sigma'_c + 0.01267D_r, R^2 = 0.888 \quad (2)$$

*For LSFd sand (Liang, 1995):*

$$\log_{10}(\delta w) = 2.529 + 0.00477\sigma'_c \quad R^2 = 0.994 \quad (3)$$

For Nevada sand (Rokoff, 1999):

$$\log_{10}(\delta w) = 3.6746 + 0.004877\sigma'_c + 0.01039D_r + 0.21802C_u - 2.1444C_c \quad R^2 = 0.819 \quad (4)$$

For LSFd sand-fines mixtures (Tao, 2003):

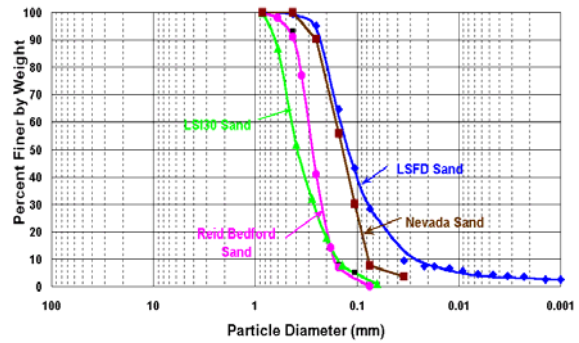
$$\log_{10}(\delta w) = 2.9760 + 0.0039\sigma'_c + 0.0027D_{rs} \quad R^2 = 0.840 \quad (5)$$

Where:  $\delta w$  = cumulative unit energy ( $J/m^3$ );  
 $\sigma'_c$  = mean effective confining pressure ( $kPa$ );  
 $D_r$  = relative density (%);  
 $R^2$  = coefficient of determination;  
 $C_u = \frac{D_{60}}{D_{10}}$  = uniformity coefficient;  
 $C_c = \frac{D_{30}^2}{D_{10}D_{60}}$  = coefficient of concavity;  
 $D_i$  = particle diameter as given by a grain-size distribution for a given percent finer denoted by the subscript  $i$ .  
 $D_{rs}$  = intergranular relative density (%).

The physical indices and classifications of RB (Reid Bedford) sand, LSI30 sand, LSFd (Lower San Fernando Dam) sand, and Nevada sand are listed in Table 1, with their corresponding particle size distributions shown in Fig. 1. The physical indices and classifications of the LSFd sand-fines mixtures are listed in Table 2, while their corresponding particle size distributions are shown in Fig. 2. In Tables 1 & 2,  $G_s$ ,  $e_{max}$ , and  $e_{min}$  refer to the specific gravity, the maximum and minimum void ratio, respectively.

Tab. 1. Physical Indices and Classifications of RB, LSI30, LSFd, and Nevada Sands

| Soils     | Reid Bedford | LSI30 | LSFD | Nevada |
|-----------|--------------|-------|------|--------|
|           | Sand         | Sand  | Sand | Sand   |
| USGS      | SP           | SP    | SM   | SP-SM  |
| $G_s$     | 2.65         | 2.66  | 2.67 | 2.66   |
| $e_{max}$ | 0.85         | 0.83  | 1.22 | 0.83   |
| $e_{min}$ | 0.58         | 0.52  | 0.71 | 0.53   |



Tab. 2. Physical Indices and Classifications of LSFd0, LSFd5, LSFd15, and LSFd28

| Soils     | LSFD0 | LSFD5 | LSFD15 | LSFD28 |
|-----------|-------|-------|--------|--------|
| USGS      | SP    | SM    | SM     | SM     |
| $G_s$     | 2.65  | 2.64  | 2.64   | 2.67   |
| $e_{max}$ | 0.949 | 0.967 | 0.962  | 1.22   |
| $e_{min}$ | 0.773 | 0.684 | 0.624  | 0.71   |

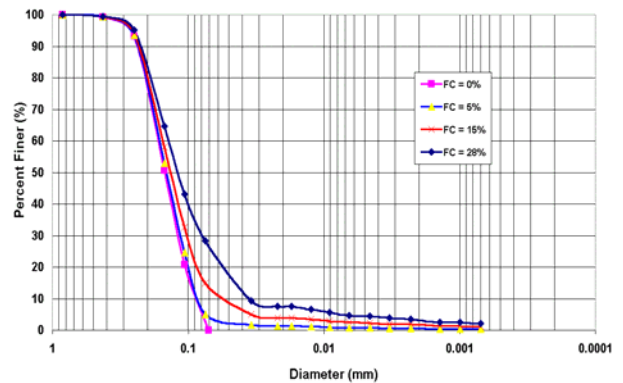


Fig. 2. Particle Size Distributions of LSFd0, LSFd5, LSFd15, and LSFd28

Then, the liquefaction resistance in terms of the unit energy can be plotted versus soil deposit depth, as shown in Fig. 4.

## 2. Determination of the amount of unit energy dissipated into the soil during the expected earthquake

It is assumed that a soil deposit is isotropic and homogeneous when subjected to earthquake action. A lumped mass model used to simulate the soil deposit at level ground is shown in Fig. 3.

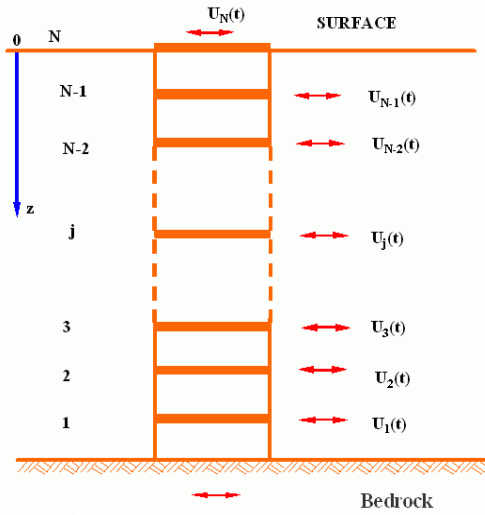


Fig. 3. Lumped Mass Model

A modified numerical procedure to calculate the seismic response of horizontal soil layers can be summarized as follows.

- Input soil properties (the unit density, initial shear modulus, and initial shear strength), degradation parameters (relating the degradation of shear modulus and shear strength with the amount of energy dissipated into soils), initial conditions, and boundary conditions;
- At the beginning of each time step, the particle velocity ( $V$ ) and displacement ( $U$ ) are known at each layer boundary;
- The shear strain can be approximated by using

$$\gamma_j = \frac{U_j - U_{j-1}}{h_j} \quad (6)$$

- The shear stress-strain curve can be constructed according to loading conditions (initial loading, unloading, or reloading).

For initial loading:

$$\tau = \frac{G_m \gamma}{1 + \frac{G_m}{\tau_f} \gamma} = f(\gamma) \quad (7)$$

Where:  $\tau$  is shear stress;  $\gamma$  is shear strain;  $G_m$  is maximum shear modulus;  $\tau_f$  is shear strength.

For unloading and reloading:

$$\frac{\tau - \tau_a}{c} = \frac{G_m \frac{\gamma - \gamma_a}{c}}{1 + \frac{G_m}{\tau_f} \left| \frac{\gamma - \gamma_a}{c} \right|} \quad (8)$$

Where  $\tau_a$  is the shear stress at the reversal point of shear stress-strain curves: either from loading changing to unloading or from unloading changing to reloading;  $\gamma_a$  is the shear strain at the reversal point of the shear stress-strain curve;  $c$  is the scale factor for the unloading and reloading branches of shear stress-strain curves, defined as:

$$c = \left| \pm 1 - \frac{\tau_a}{\tau_f} \right|$$

Where: the first term is positive for reloading and negative for unloading.

- The displacement of the  $j^{\text{th}}$  layer at time  $t + \Delta t$  can be calculated by solving Eq. (9).

$$m_j \ddot{U}_{j,t+\Delta t} = \tau_{j,t} - \tau_{j+1,t} = f(\gamma_{j,t}) - f(\gamma_{j+1,t}) \quad (9)$$

$$= F(U_{j-1,t}, U_{j,t}, U_{j+1,t})$$

- Calculate the dissipated unit energy,  $\delta W_j^n$ , from  $\tau_j^n$  and  $\gamma_j^n$ , due to the EW (East-West) component and the NS (North-South) component, individually, and add them up;
- The sum of the dissipated unit energy from the previous step is used to update the shear modulus and the shear strength using Eqs. (10) & (11) at each reversal loading point;

$$\begin{cases} G_{mt} = G_{m0} \left( 1 - A_1 \frac{\delta W}{\sigma'_c} \right) & G_{mt}/G_{m0} \geq 0.9 \\ G_{mt} = G_{m0} \left( 1 - A_2 \frac{\delta W}{\sigma'_c} - B_2 \right) & G_{mt}/G_{m0} < 0.9 \end{cases} \quad (10)$$

$$\begin{cases} \tau_{ft} = \tau_{f0} \left( 1 - A_1 \frac{\delta W}{\sigma'_c} \right) & \tau_{ft}/\tau_{f0} \geq 0.9 \\ \tau_{ft} = \tau_{f0} \left( 1 - A_2 \frac{\delta W}{\sigma'_c} - B_2 \right) & \tau_{ft}/\tau_{f0} < 0.9 \end{cases} \quad (11)$$

- Repeat the above steps until the earthquake is over.

The shear stress and shear strain time histories at the depth of interest can be obtained from the aforementioned numerical procedure. The cumulative dissipated unit energy can be easily calculated from the hysteretic loops. Finally, the variation of the dissipated unit energy with depth can be plotted, as shown in Fig. 4.

### 3. Determination of the liquefaction potential

The liquefaction potential of a soil deposit can be predicted by comparing curves A and B in Fig. 4. Liquefaction would be expected in the zone of the deposit where curve B is to the right of Curve A. On the basis of the pore pressure-energy relationship developed by Wallin (2000), the time histories of

pore pressure build-up at a certain depth can also be plotted and used to confirm the liquefaction evaluation made from the point view of the unit energy concept. Furthermore, the degradation of the shear modulus and shear strength is also effective indicator of liquefaction occurrence.

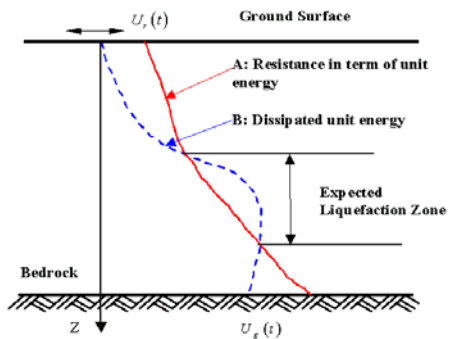


Fig. 4. Determination of the Liquefaction Potential of a Soil Deposit Using the Energy Method

### FIELD CASE VERIFICATION

Two downhole array data recorded at the Wildlife site during the 1987 Superstition Hills earthquake and the 1987 Elmore Ranch earthquake were used to verify the aforementioned energy-based procedure.

The Wildlife site consists of a loose silt surface layer down to a depth of 2.5 m, a loose silty-sand layer between 2.5 m and 6.8 m, and a stiff to very stiff silty-clay layer from 6.8 m to about 11.5 m based on the in situ and laboratory investigations (Bennett et al. 1984; Hagg 1985). The ground water table was at about 1.5 m in depth. The movements of the soil deposit during these earthquakes were monitored by installing two accelerometers at the ground surface and at a depth of 7.5 m, respectively. The recorded acceleration time series at a depth of 7.5 m during these two earthquakes were chosen as input excitation. Their EW (East-West) and NS (North-South) components are shown in Figs. (5) & (6), respectively. The values of parameters used in the analysis are listed in Table 3.

Table 3. Values of Parameters Used in the Analysis

| Layer No. | H (m) | $G_{m0}$ (kPa) | $\tau_{f0}$ (kPa) | $A_1$ | $A_2$ | $B_2$ |
|-----------|-------|----------------|-------------------|-------|-------|-------|
| 1         | 1.0   | 46491.48       | 46.49             | 380   | 10    | 0.84  |
| 2         | 1.0   | 39261.60       | 39.26             | 400   | 10    | 0.84  |
| 3         | 1.0   | 32749.92       | 32.75             | 440   | 10    | 0.84  |
| 4         | 1.0   | 30643.20       | 30.64             | 460   | 10    | 0.84  |
| 5         | 1.0   | 25711.56       | 25.71             | 480   | 10    | 0.84  |
| 6         | 1.0   | 19008.36       | 19.01             | 485   | 10    | 0.84  |
| 7         | 1.5   | 16710.12       | 16.71             | 400   | 10    | 0.84  |

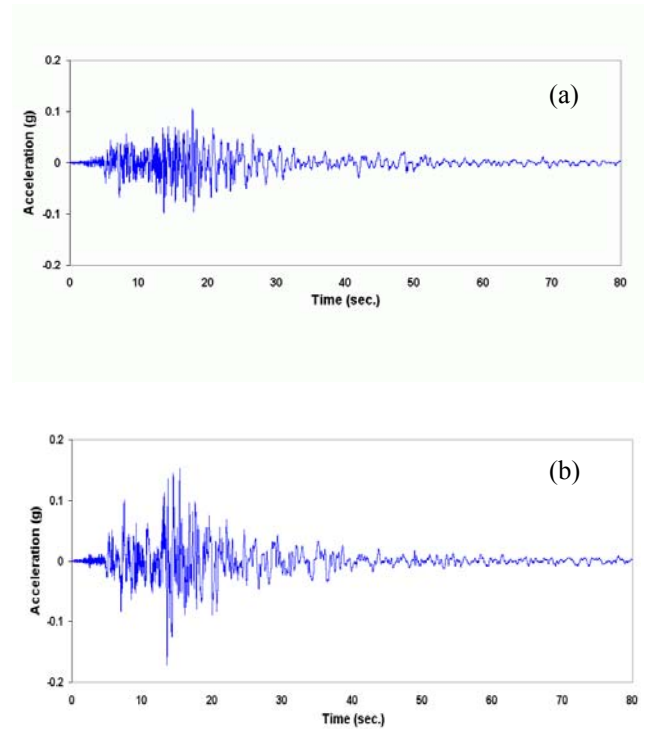


Fig. 5 Recorded Acceleration Time Series at a Depth of 7.5 m at the Wildlife Site (During the 1987 Superstition Hills Earthquake) (a) EW; (b) NS

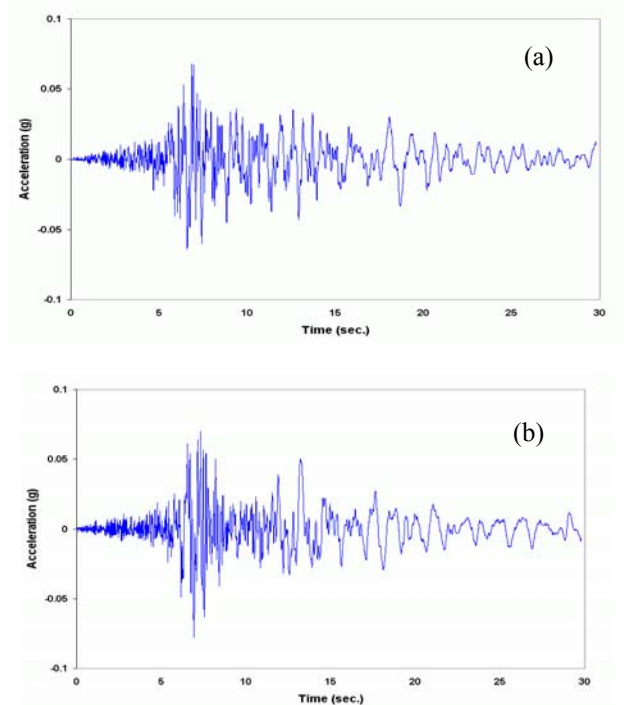


Fig. 6 Recorded Acceleration Time Series at a Depth of 7.5 m at the Wildlife Site (During the 1987 Elmore Ranch Earthquake) (a) EW; (b) NS

The liquefaction susceptibility of the soil deposit during the 1987 Superstition Hills earthquake can be determined from Fig. (7). It can be seen from this figure that a liquefied zone at depths of 3 m to 5.5 m would be expected. This prediction is in good agreement with field observations.

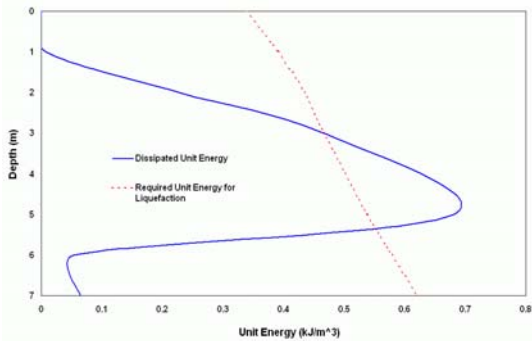
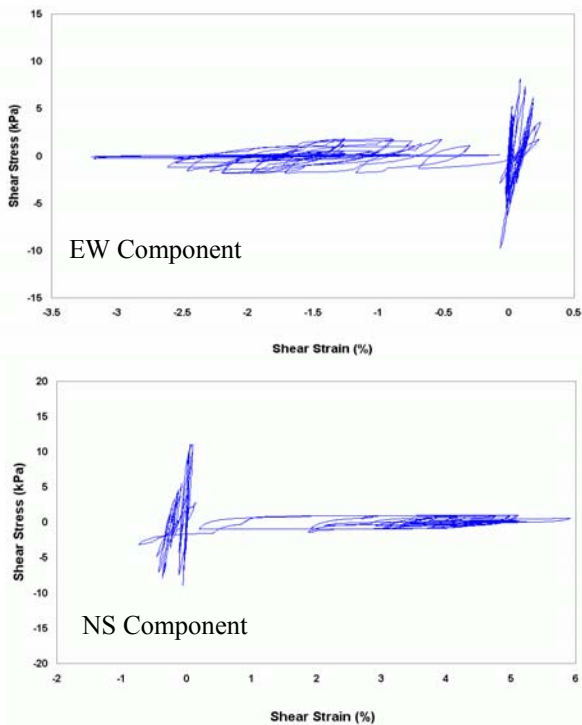


Fig. 7 Determination of the Liquefaction Potential of the Soil Deposit at the Wildlife Site During the 1987 Superstition Hills Earthquake

The calculated shear stress-strain relationships for the EW and NS component at a depth of 3.0 m during the 1987 Superstition Hills earthquake are shown in Fig. (8), respectively. The flat cycles of the calculated shear stress-strain curves also indicates the occurrence of liquefaction at a depth of 3.0 m.



An energy-based pore pressure model (Wallin 2000) to calculate the build-up of pore pressure is given in Eq. (12):

$$\frac{u}{\sigma'_v} = 3.91703\delta W - 5.07623\delta W^2 + 2.08714\delta W^3 \quad R^2 = 0.984 \quad (12)$$

The good agreement between the calculated and measured pore pressure time histories at a depth of 3.0m, as shown in Fig. (9), confirms the validity of the energy-based pore pressure model.

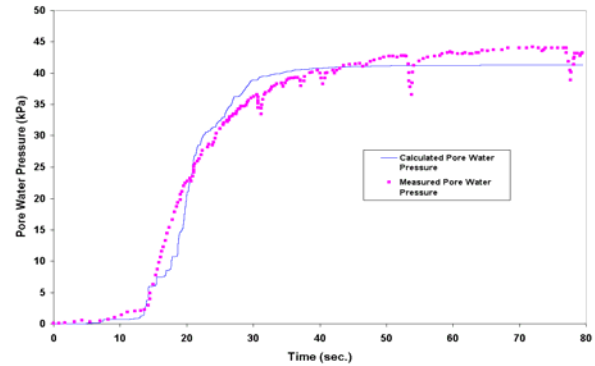


Fig. 9 Comparison of the Calculated and Recorded Pore Water Pressure Time Histories at a Depth of 3.0 m at the Wildlife Site During the 1987 Superstition Hills earthquake

### Effects of Multi-Dimensional Loading

The dissipated unit energy at a depth of 3.0 m during the 1987 Superstition Hills earthquake due to the one-dimensional and two-dimensional analyses are shown in Fig. (10). It can be seen that the dissipated unit energy from the two-dimensional analysis is substantially larger than from the one-dimensional analysis. It is also found that the dissipated unit energy from the two-dimensional analysis is larger than the sum of two one-dimensional analyses (due to the EW or NS components). These observations coincide with those by Zienkiewicz (Zienkiewicz et al., 1999). Therefore, it can be concluded that both horizontal components of earthquake loading are significant to the development of liquefaction and pore water pressure buildup, and should be considered together.

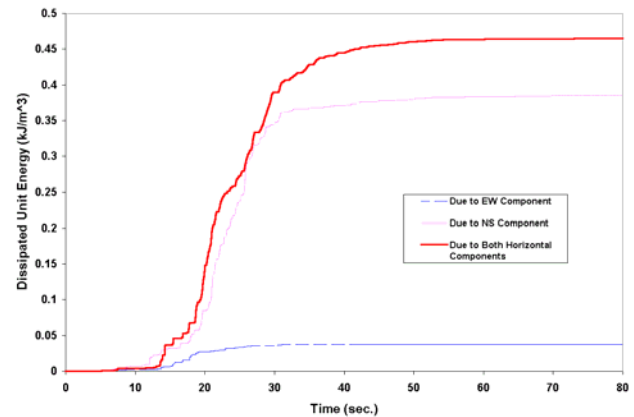


Fig. 10 Comparison of Dissipated Unit Energy due to EW Component, NS Component, and Both Horizontal Components at a Depth of 3.0 m at the Wildlife Site During the Superstition Hills Earthquake

## The 1987 Elmore Ranch earthquake

The NS component of the calculated shear stress-strain relationships at a depth of 3.0 m during the 1987 Elmore Ranch shown in Fig. (11) generally agrees with that calculated by Zeghal (Zeghal et al. 1994). This plot indicates that the soil remains stiff and no liquefaction developed during this earthquake, as it was confirmed at the instrumented site.

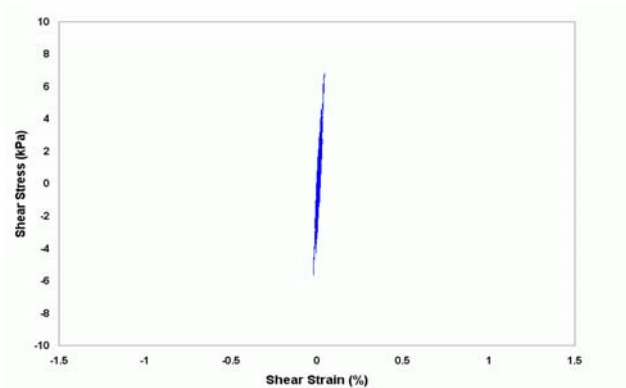


Fig. 11 Calculated Shear Stress-Strain Curves at a Depth of 3.0 m at the Wildlife Site During the 1987 Elmore Ranch Earthquake

## Discussion of Degradation Parameters

The same degradation parameters were used for the Wildlife site during the 1987 Superstition Hills earthquake and the 1987 Elmore Ranch earthquake. It can be seen from the above analysis that degradation parameters are mainly dependent on the characteristics of soils and sites features, and relatively insensitive to the loading features.

## CONCLUSIONS

The successful field verification presented in this paper provides strong evidence in favor of the energy-based procedure to determine the liquefaction potential of soil deposits. The significance of both horizontal components of earthquake loading is confirmed by the comparative study presented herein. It has also been found that degradation parameters are mainly soil-dependent. However, more field case studies are required to examine the energy-based procedure and to develop more generalized degradation parameters.

## REFERENCES

Bennett, M.J., McLaughlin, P.V., Sarmiento, J.S., and Youd, T.L. [1984]. "Geotechnical investigation of liquefaction sites,

Imperial Valley, California." *Open-file Rep. 84-252*, U.S. Geological Survey, Washington, D.C.

Haag, E.D. [1985]. "Laboratory investigation of static and dynamic properties of sandy soils subjected to the 1981 Westmoreland earthquake." *Rep. GR85-11*, Geotechnical Engineering Center, The University of Texas at Austin, Austin, Tex.

Liang, L. [1995]. "Development of an energy method for evaluating the liquefaction potential of a soil deposit." Ph.D. Dissertation, Department of Civil Engineering, Case Western Reserve University, OH.

Liang, L., Figueroa, J.L., and Saada, A.S. [1995]. "Liquefaction under random loading: unit energy approach." *J. Geotech. Engrg. Div.*, ASCE, 121(11), 776-781.

Wallin, M.S. [2000]. "Evaluation of normalized pore water pressure vs. accumulating unit energy relationship for determining liquefaction potential of soils." M.S Thesis, Department of Civil Engineering, Case Western Reserve University, OH.

Tao, M. [2003]. "Case history verification of the energy method to determine the liquefaction potential of soil deposits." Ph.D. Dissertation, Department of Civil Engineering, Case Western Reserve University, OH.

Tao, M., Figueroa, J.L., and Saada, A.S. [2003]. "Interpretation of Cyclic Simple Shear and Cyclic Triaxial Tests in Terms of the Unit Energy." Submitted for review.

Zeghal, M., and Elgamal, A.W. [1994]. "Analysis of site liquefaction using earthquake records." *J. Geotech. Engrg.*, ASCE, 120(6), 996-1017.

Zienkiewicz, O.C., Chan, A.H.C., Pastor M., Schrefler B.A., and Shiomi, T. [1999]. *Computational geomechanics with special reference to earthquake engineering*. John Wiley & Sons.